Original Article

Spatial matching and flow in supply and demand of water provision services: A case study in Xiangjiang River Basin

DENG Chu-xiong[1,2#] https://orcid.org/0000-0001-7979-9799; e-mail: dcxppd@hunnu.edu.cn

ZHU Da-mei[1,2#] https://orcid.org/0000-0002-5162-7087; e-mail: zdm1215@hunnu.edu.cn

LIU Yao-jun[1,2*] https://orcid.org/0000-0003-2482-3784; ✉ e-mail: liuyj461@163.com

LI Zhong-wu[1,2,3*] https://orcid.org/0000-0002-3219-0027; ✉ e-mail: lzw17002@hunnu.edu.cn

* Corresponding author

 # Two authors contributed equally to this work and should be considered co-first authors.

1 College of Resources and Environmental Sciences, Hunan Normal University, Changsha 410081, China

2 Hunan Key Laboratory of Geospatial Big Data Mining and Application, Changsha 410081, China

3 College of Environmental Science and Engineering, Hunan University, Changsha 410082, China

Abstract: Global climate change and increased human consumption have aggravated the uneven spatiotemporal distribution of watershed water resources, affecting the water provision supply and demand state. However, this problem has often been ignored. The present study used the Xiangjiang River basin (XRB) as the study area, and the Integrated Valuation of Ecosystem Services and Trade-offs (InVEST) model, demand quantification model, supply–demand ratio, and water flow formula were applied to explore the spatial heterogeneity, flow, and equilibrium between water supply and demand. The results demonstrated significant spatial heterogeneity in the upstream, midstream, and downstream regions. The areas of water shortage were mainly located the downstream of the Changsha–Zhuzhou–Xiangtan urban agglomeration, and the Hengyang basin was the most scarcity area. Affected by terrain gradients and human needs, water flow varied from -16.33×10^8 m^3 to 13.69×10^8 m^3 from the upstream to the downstream area, which provided a possibility to reduce spatial heterogeneity. In the future, measures such as strengthening water resource system control, sponge city construction, and dynamic monitoring technology should be taken to balance the supply and demand of water in different river sections of the basin. This study can provide references for regulating water resources allocation in different reaches of the basin.

Keywords: Water provision services; Supply and demand; Spatiotemporal dislocation; Water flow; Water management and saving policy; Xiangjiang River basin

1 Introduction

Ecosystems generate a range of goods and services necessary for human well-being, collectively

referred to as ecosystem services (Nelson et al. 2009). Ecosystem services have become a critical indicator for measuring ecosystem quality and sustainability since the Millennium Ecosystem Assessment. The supply of ecosystem services is understood as services that the ecosystem can provide for human society, while the demand for ecosystem services is understood as the sum of all ecosystem goods and services currently consumed or used in a particular area over a given period (Villamagna et al. 2013). According to the Economics of Ecosystems and Biodiversity (TEEB), the economic activities of stakeholders result in a huge demand for ecosystem services and lead to changes in the status of ecosystem services. The supply and demand of ecosystem services can directly affect the stability of the regional ecosystem. The imbalance between the two leads to a series of ecological problems, such as biodiversity loss, soil erosion, and ecological degradation, which aggravate the risk of benign ecosystem reversal, and disrupt the relationship between the supply and demand of ecosystem services increasingly. Therefore, understanding the relationship between the supply and demand of ecosystem services and analyzing their matching status are of great practical significance to realize the sustainable development of the social economy and regional ecological security.

Driven by natural and man-made factors, ecosystem service flow is a spatiotemporal transfer of ecosystem services from the source area (provision area) to the utilization region (benefiting area) (Bagstad et al. 2013, Schroter et al. 2014). Essentially, water flow research is used to quantitatively evaluate and establish the spatiotemporal relationship between water supply and demand (Fu et al. 2015) and then provide ideas for ecological compensation and management optimization. In recent years, ecosystem service flows have received increasing attention worldwide. The research foci can be divided into three categories: defining an ecosystem service, balance between supply and demand, and spatiotemporal delivery (Baró et al. 2016; Vigl et al. 2017). Various conceptual systems and classifications have been established depending on the flow direction or the mobility of the supply benefit area (Villamagna et al. 2013, Baró et al. 2016, Vigl et al. 2017). Spatial matching of supply and demand is a major obstacle in ecosystem service flow research (Bagstad et al. 2014). Some studies have indicated that land use and land cover change (LUCC) will have a significant impact on the availability of water resources (Brauman et al. 2007, Palomo et al. 2014). An increase in vegetation leads to a decrease in annual average discharge by increasing evapotranspiration (Ben et al. 2016, Xu et al. 2018), whereas urban expansion leads to an increase in runoff by decreasing infiltration (Farley et al. 2005, Feng et al. 2016). Owing to the spatial heterogeneity of ecosystems, regions with high supply capacity may not be in line with the location of the main benefiting area, which causes a mismatch between water supply and demand (Serna-Chavez et al. 2014, Song et al. 2015, Chen et al. 2017). However, to date, few assessments have considered the spatial flow between the supply and demand of water provision. Therefore, to optimize water resource management, it is crucial to address this issue.

Watersheds are complicated systems composed of water resources, ecological environment, and socioeconomic environment and have significant spatial heterogeneity and imbalance among the intrinsic elements. Insufficient water supply is observed against the backdrop of global warming and expanding urbanization, even in humid monsoon areas with high precipitation and water demand. The Xiangjiang River Basin (XRB), an area characterized by large amount of rainfall and rapid urbanization and a vital tributary of the Yangtze River basin, is confronted with large-scale soil and water loss, frequent droughts and floods, and water security challenges. However, little is known about these challenges, and studying them would provide a reference for optimizing water resource allocation and promoting the development of a social economy in the watershed. Therefore, we used the XRB as the area of the case study and used the Integrated Valuation of Ecosystem Services and Tradeoffs (InVEST) model, supply–demand ratio, and water flow formula to comprehensively explore the spatial heterogeneity and flow between supply and demand of water provision. The results provide a basis for optimizing water resource management and ecological compensation.

2 Materials and Methods

2.1 Study area

The Xiangjiang River is an important river in Hunan Province, southern China, which originates

from Xing'an County in Guangxi Province, flows from south to north, and discharges into Dongting Lake. The XRB (110°30'–114°30'E, 24°30'–28°40'N), an area of approximately 9.47 × 10⁴ km², is located in the midstream of the Yangtze River, which accounts for 40% of the whole area and 60% of the population of Hunan Province. The area generates 75% of the gross domestic product (GDP, 2018), and industrialization and agricultural intensification have significantly increased the water demand. The study region covers nine municipalities in Hunan Province (Fig. 1). The dominant land cover is forest, which accounts for more than 60% of the surface area. The topography of the XRB is domina ted by low mountains and hills with a subtropical monsoon climate. The annual mean temperature is approximately 17°C, and the annual mean precipitation ranges from 1,200 to 1,700 mm, unevenly distributed, with 60%–70% of the precipitation occurring during the flood season (March to July), whereas precipitation from November to February accounts for less than 15% of the total precipitation. The level of urbanization has increased in the downstream as compared to the upstream of XRB. However, the integrated development of the Changsha–Zhuzhou–Xiangtan (CZX) urban agglomeration has led to a rapid increase in water demand and prominent supply–demand contradiction. Therefore, a precise assessment of supply and demand in the XRB is of high importance for water resource planning and management.

2.2 Modeling approach for water supply calculation

The water yield module of the InVEST model version 3.6.0, based on the water balance principle, is a widely used simulation method for supplying water provision services (Boithias et al. 2014, Verhagen et al. 2017, Zhang et al. 2017), which has been widely recognized and applied.

2.2.1 InVEST model algorithm

The annual water yield module runs on a gridded map and quantifies the water supply in each pixel. The equation is as follows:

$$Y_x = \left(1 - \frac{\text{AET}_x}{P_x}\right) \times P_x \tag{1}$$

where, AET_x is the actual evapotranspiration for pixel x, and P_x is the annual precipitation on pixel x.

AET_{xj} and P_x are based on the Budyko curve (Budyko 1974) and evaluated explicitly on pixel x using the following equation:

$$\frac{\text{AET}_x}{P_x} = 1 + \frac{\text{PET}_x}{P_x} - \left[1 + \left(\frac{\text{PET}_x}{P_x}\right)^\omega\right]^{1/\omega} \tag{2}$$

where, PET_x is the potential evapotranspiration for pixel x on landscape j, and can be calculated as follows:

$$\text{PET}_x = K_c(\varepsilon_x) \times \text{ET0}(x) \tag{3}$$

where, $K_c(\varepsilon_x)$ is the vegetation evapotranspiration coefficient linked to the land-use type in each pixel. $\text{ET0}(x)$ is the reference evapotranspiration for pixel x,
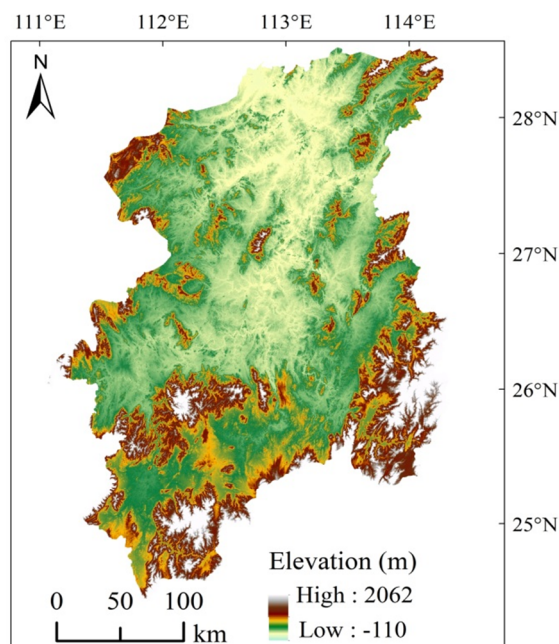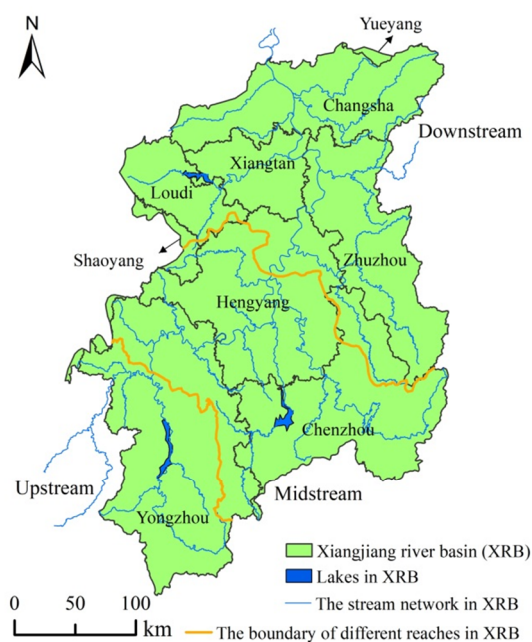

Fig. 1 Maps of scope and elevation gradient of Xiangjiang River Basin, in Hunan Province, southern China

which is obtained using the Hargreaves equation (Li et al. 2017) as follows:

$ET_0(x)$

$=0.0023 \times R\alpha \times [(T_{max}+T_{min})/2+17.8] \times (T_{max}+T_{min})^{1/2}$ (4)

where, $R\alpha$ is extraterrestrial radiation (MJ m^{-2} d^{-1}), and T_{max} and T_{min} are the mean maximum and minimum temperatures, respectively, in °C.

$\omega(x)$ is a nonphysical parameter that characterizes natural climatic soil properties and is calculated as follows:

$$\omega(x)=Z(\frac{PAWC_x}{P_x})+1.25 \qquad (5)$$

where, the plant-available water capacity (PAWC) is calculated as the difference between the wilting point and field water holding capacity on pixel x, and Z is an empirical factor that denotes the native precipitation and extra hydrogeological characteristics (Xu et al. 2018), which are positively correlated with the number of rainfall events (N) per year ($Z = 0.2N$).

2.2.2 Model data input and processing

Seven maps are required to operate the water yield module: precipitation, ET0 , depth to root restricting layer, plant available water fraction, land use, watersheds, and biophysical coefficients (Table 1). All the data were resampled at a spatial resolution of 30 m and the projected coordinate system of the World Geodetic System 1984.

Table 1 Biophysical table used for running the InVEST model, providing information on vegetation, plant evapotranspiration coefficient Kc, and root depth for each land use and land cover change (LUCC) class.

No.	LUCC description	LUCC vegetation	Kc	Root depth (mm)
1	Forest	1	1.00	3,500
2	Cropland	1	0.65	2,000
3	Built_up area	0	0.30	1
4	Grassland	1	0.65	2,400
5	Water bodies	0	1.10	1
6	Unused land	0	0.50	1

Meteorological data, including temperature, precipitation, and radiation data, were acquired from the China National Network Information Center (http://data.cma.cn/) and spatially interpolated according to the kriging algorithm (Fig. 2a). The annual potential evapotranspiration was calculated using the Hargreaves equation for each station (Fig. 2b).

The land use layers were obtained from the Resource and Environment Science and Data Center (RESDC) (http://www.resdc.cn). In this study, land

use data from the XRB in 2015 were aggregated into six land use types according to the Chinese Academy of Sciences land resources classification system (Zhang et al. 2014) (Fig. 2c): forest (67.8%), cropland (26.3%), grassland (2.6%), built-up area (1.7%), water bodies (1.4%), and unused land (0.2%), including saline−alkaline and bare land. PAWC can be estimated based on the physical and chemical properties of soil (Sharp et al. 2018), where a gridded map of soil depth (mm) and soil texture was generated. Based on the second soil survey database, which was downloaded from the Cold and Arid Regions Science Data Center at Lanzhou (ftp://ftp2.westgis.ac.cn/) (Fisher et al. 2008), the equation is as follows:

$PAWC=54.509-0.132 \times SAND-0.003 \times SAND^2$

$-0.055 \times SILT-0.006 \times SILT^2-0.738 \times CLAY$

$+0.007 \times CLAY^2-2.688 \times SOC+0.501 \times SOC^2$ (6)

where, SAND, SILT, CLAY, and SOC are the proportions of sand, silt, clay, and organic matter in the soil, respectively. The data were converted to fractions from 0 to 1 according to the input requirements (Fig. 2d). The layers of soil depth and texture were acquired from the Harmonized World Soil Database (Liu et al. 2005).

The parameter Z, as a seasonal climatic factor, captures the precipitation distribution and hydrogeological characteristics, with a possible value varying from 1 to 30, and is positively correlated with the rainfall frequency. The constant can be calculated as 0.2N, where N is the number of rainfall events ($N >$ 1 mm) per year (Zhou et al. 2005). In this study, N was calculated based on yearly precipitation from observation stations, and Z was set to eight after multiple revisions based on previous research and application (Fisher et al. 2008).

The biophysical coefficients of each LUCC class used in the model are listed in Table 1.

Root depth refers to the maximum depth that plant roots can extend in the soil due to different physical and chemical characteristics of the environment (Fig. 2e). For vegetated LUCC, the root depth was determined as described (Redhead et al. 2016). If the LUCC$_{veg}$ information was included, the value was set as 1, and if the LUCC$_{veg}$ information was not included, the value was set as 0. Kc is the plant evapotranspiration coefficient based on the UN Food and Agriculture Organization (FAO) Irrigation and Drainage Paper 56 guidelines (Yang et al. 2019).

2.2.3 Model calibration and verification

Based on the data prepared above, the model was run to obtain the annual spatial distribution of the water supply. We then compared the simulated annual total water yield against the statistical data from the Water Resources Bulletin of Hunan Province (2015) using the determination coefficient R-squared (R^2), root mean squared error (RMSE), and Nash–Sutcliffe efficiency coefficient (NSE) to calculate the validation. The simulation results showed an excellent fitting effect and high reliability of the water yield model ($R^2 = 0.8698$, Prob < 0.5, $n = 9$, RMSE = 72.31 × 10^8 m³, NSE = 0.9975), which is similar to the results obtained by Fisher et al. ([2008]). The equations are as follows:

$$R^2 = \frac{\sum_{i=1}^{n}(sta_i - sta_{avg})(simu_i - simu_{avg})}{\sqrt{\sum_{i=1}^{n}(sta_i - sta_{avg})^2}\sqrt{\sum_{i=1}^{n}(simu_i - simu_{avg})^2}} \quad (7)$$

$$RMSE = \sqrt{\frac{\sum_{i=1}^{n}(sta_i - simu_i)^2}{n}} \quad (8)$$

$$NSE = 1 - \frac{\sum_{i=1}^{n}(sta_i - simu_i)^2}{\sum_{i=1}^{n}(sta_i - sta_{avg})^2}, \ NSE \leq 1 \quad (9)$$

where, Sta_i, $Simu_i$, Sta_{iavg}, $Simu_{iavg}$ represent the observed value, simulation result, average observed value, average simulated result in municipality i, respectively, and n represents the number of administrative units. R^2 was used to evaluate the degree of fit between the measured and simulated values. The closer R^2 is to 1, the better the simulation degree. If $R^2 = 1$, the simulated and measured values were equal. RMSE reflects the deviation between the observed and true values. NSE is an important parameter used to evaluate model quality and is generally used to verify the simulation results of hydrological models. If the NSE value is close to 1, the model is of good quality and high reliability, and if the
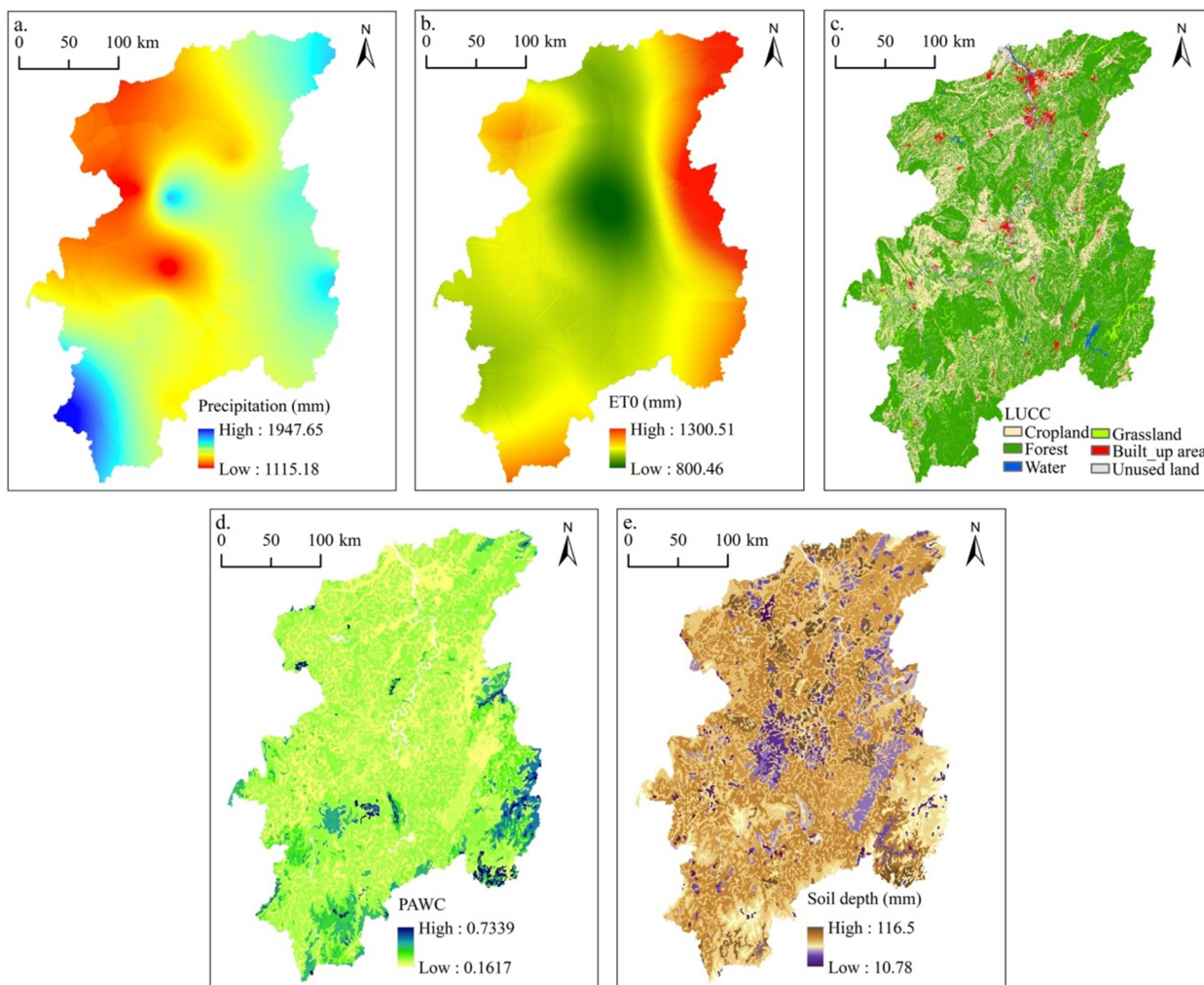

Fig. 2 Input data for Xiangjiang River basin (XRB) for 2015. (a) Mean annual precipitation; (b) Potential evapotranspiration (ET0); (c) land use and land cover change (LUCC); (d) Plant-available water capacity (PAWC); (e) Soil depth.

NSE value is close to 0, the simulation results are close to the average level of the observation values, and the overall result is credible. If the NSE value is significantly less than zero, the model is unreliable.

2.3 Quantification of demand

Water demand refers to the water consumption for living, production, and other activities, and it indicates the spatial distribution characteristics of anthropogenic water demand (Canadell et al. 1996; Zhang et al. 2017; Xu et al. 2018). According to the definition and classification of water consumption in the ARIES model (Baró et al. 2016), the demand for water provision mainly includes four categories: agricultural, industrial, domestic, and livestock. Combined with the reality of the study area, agricultural water (AWC), industrial water (IWC), domestic water (DWC), urban public water (UWC), and ecological environment water (EWC) consumption was used to assess the demand for water provision services (water consumption), and data were obtained from the Water Resources Bulletin of Hunan Province (2015). The total water consumption (TWC) in each municipality was calculated by adding the five categories using the following equation:

$$\text{TWC}=\text{AWC}_i + \text{IWC}_i+\text{DWC}_i + \text{UWC}_i+ \text{EWC}_i \quad (10)$$

where, TWC represents the total water consumption, and AWC_i, IWC_i, DWC_i, UWC_i, EWC_i represent the water consumption of agriculture, industry, residents, urban public, and ecological environment in municipality$_i$, respectively.

2.4 Spatial heterogeneity of supply and demand

2.4.1 Mismatches in water supply and demand

Spatial matching of water supply and demand is a precondition and the foundation of optimal regional water resource spatial allocation. In this study, to describe the mismatches, the water supply and demand ratio (WSDR) was used to evaluate the regional water balance (Li et al. 2017; Zhang et al. 2017), and to reveal the surplus or deficiency of water resources (Farley et al. 2005; Verhagen et al. 2017). The calculation formula is as follows:

$$\text{WSDR}=\frac{S_i-D_i}{(S_{imax}+D_{imax})/2} \quad (11)$$

where, WSDR represents the state of supply and demand, and the value range is [−1,1]. S_i and D_i refer to the supply and demand in municipality i, S_{imax} and D_{imax} are the maximum supply and demand in municipality i, respectively. A positive WSDR indicates a benefiting area with water surplus, and a negative WSDR represents a benefitting area with insufficient supply, and a zero value indicates balance between supply and demand.

2.4.2 Spatial flow of water supply and demand

Topography-induced gravity and human needs were regarded as the main drivers of water flows (Allen et al. 1998; Qin et al. 2019); river courses usually were taken as transfer channels to generate directional service flows from upstream to downstream.

First, we defined the provision (WSDR>0) and benefiting area (WSDR<0) based on the results of Section 2.4.1; second, based on DEM data in the study area, ArcGIS hydrological analysis tools were used to extract streams by filling depressional land, flow direction analysis, flow rate analysis, river network analysis, river classification, and vectorization of the raster river network. Finally, according to the hydrological connectivity of the river, the water provision service flow was driven by the "water flowing to the lower part" caused by the gravity difference between the high and the low terrain, the path of the water service flow was determined by the river system network, and the flow was determined by the surplus of water supply in the basin to flow from upstream to downstream.

Owing to the vast differences between water flows in different river sections, and the limitations in data and technical conditions, water flow in this study only referred to the relationship between the ideal supply and the benefit zone and did not consider obstacles and resistance. This was defined as follows:

$$\text{Flow}_i=\text{WS}_i - \text{WU}_i \times \text{WC}_{ci} \quad (12)$$

The benefiting and provision areas were connected by flow size and direction. The flows were the entire margin that consumed water from the local water supply. WS_i and WU_i refer to the water supply and water use in municipality i, respectively, and WC_{ci} indicates the water consumption coefficient in municipality i.

2.4.3 Calculation of the water security index

The water security index (WSI), as a metric of water security, is calculated by modifying the WSDR

(Boithias et al. 2014). As there are significant differences in flow in different river sections, we use logarithmic transformation to make the water security index of the basin more visual and comparative. It could be calculated as follows:

$$\text{WSI} = \log_{10}\left(\frac{S_i}{D_i}\right) \tag{13}$$

where, S_i and D_i refer to the supply and demand in municipality i. An WSI value greater than 0 indicates a water provision service surplus; a value less than 0 indicates a water provision service deficit.

3 Results

3.1 Changes in the supply of water provision

The average water yield of the nine urban units in the XRB was calculated as shown in Fig. 3a. There was high spatial heterogeneity in the average water yield between the different urban units. The upstream area, such as Yongzhou, had the highest water yield capability (1,120.01 mm), and its capability decreased downstream, with the lowest average water yield found in Yueyang (245.22 mm). The surface area of the CZX urban agglomeration downstream is similar to that in Yongzhou, whereas the total water yield of CZX, accounting for 41.27% of the basin area, was 3,015.71 mm, which was 35% higher than that of Yongzhou. Furthermore, the surface areas of Shaoyang, Hengyang, and Chenzhou, located midstream, were approximately twice that of CZX, whereas the total water yield was 2,495.66 mm, which was 17.24% lower than that of CZX. This could be

explained by the high level of urbanization in CZX and the numerous impervious surfaces that sharply decrease rainfall infiltration, which is beneficial for runoff generation. The lower water yield in Shaoyang and Loudi was partly due to forest coverage, which promoted increased evaporation and soil water holding capacity.

3.2 Changes in the demand of water provision

The total water consumption and water use structures are shown in Fig. 3b. There was a high spatial homogeneity in water demand between the different urban units. The downstream area, such as Changsha, had the highest value (37.37×10^8 m³), accounting for 19.57% of the total water consumption. The urbanization level had a notable impact on water demand, and water demand decreased upstream. The upstream area, such as Yongzhou, with a value of 25.22×10^8 m³, accounted for 13.21% of the total water consumption, which was 22% lower than that of the midstream areas. The midstream areas, including Hengyang, Chenzhou, and Shaoyang, had a water consumption value of 67.54×10^8 m³, and the downstream area, such as the CZX urban agglomeration, had a value of 81.78×10^8 m³, accounting for 42.8% of the total water consumption, which was 7% higher than that of the midstream areas. This could be explained mainly by the differences in economic development and terrain gradients.

There were also significant differences in the water use structure between the different urban units (Fig. 4). Midstream areas, such as Hengyang, had the
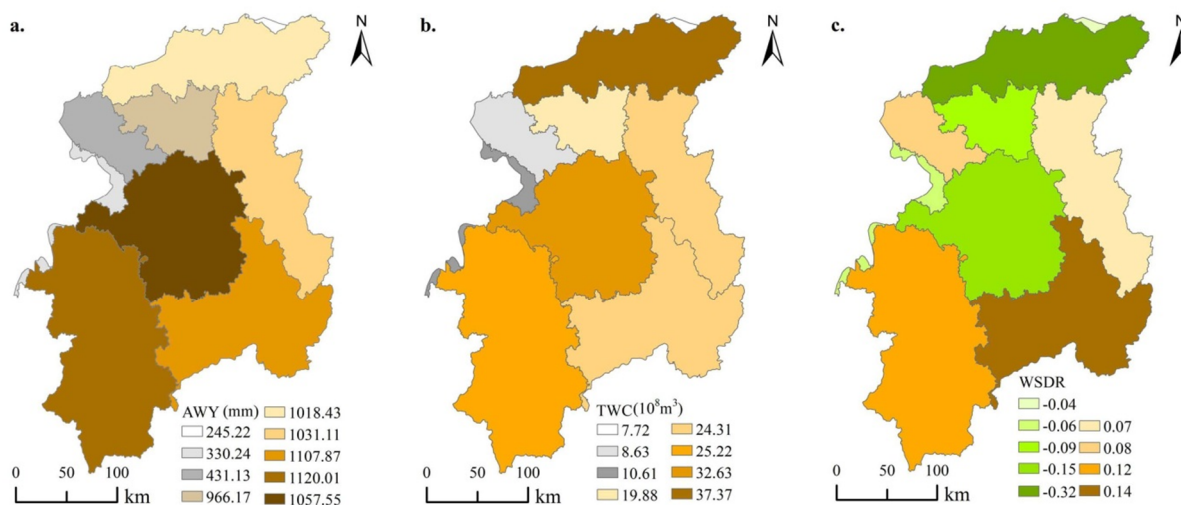

Fig. 3 Supply, demand and supply–demand ratio of water resources in different urban units. (a) Average water yield (AWY); (b) Total water consumption (TWC); (c) Water supply–demand ratio (WSDR) to reflect the matching degree.

highest proportion of AWC (19.26%), whereas upstream areas, such as Changsha, had the highest proportion of IWC, RWC, UWC, and EWC, with values of 22%, 21.6%, 43.9%, and 36%, respectively. Industrial structure had a significant impact on the water use. EWC and UWC were the main water demands in downstream areas, such as the CZX urban agglomeration, accounting for 62.15% and 62.85%, respectively, and AWC (38.15%) was the primary demand in midstream areas, such as Hengyang, Chenzhou, and Shaoyang. The DWC was the main water demand in the upstream areas, such as Yongzhou.
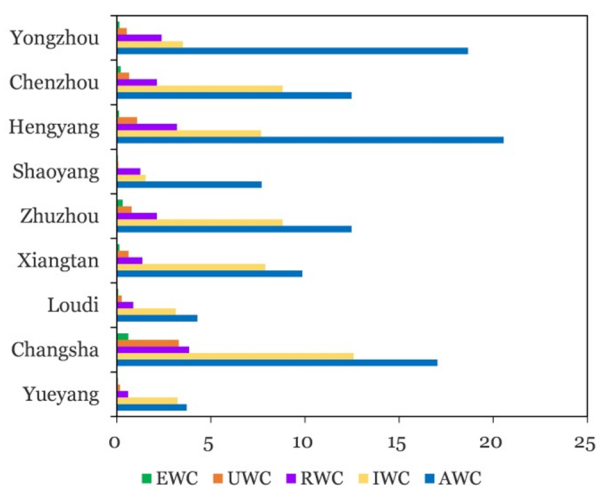

Fig. 4 Water consumption structure of the urban units in XRB. EWC, UWC, RWC, IWC, AWC represents the water consumption of ecological environment, urban public, residents, industry, agriculture in municipality of XRB, respectively.

3.3 Mismatches between supply and demand

The WSDR of the nine urban units in the XRB was calculated as shown in Fig. 3c. There was a conspicuous spatial mismatch between supply and demand. The downstream areas, such as Changsha and Xiangtan, were in short supply and had a negative WSDR, which could mainly be explained by the lower annual precipitation and integrated development of CZX. The WSDR in the upstream areas, such as Yongzhou and Chenzhou, was greater than 0, indicating that supply exceeded the demand, which was mainly attributed to soil and water conservation projects and less human intervention. Additionally, it is noteworthy that the WSDR of Hengyang, located midstream was less than 0 (-0.15), which is attributed

to the high population density and an old industrial structure.

3.4 Spatial flow of water supply and demand

According to the balanced characteristics of the water supply and demand, the obvious water service flow among the nine administrative regions is mapped in Fig. 5. The regions whose water supply cannot meet the actual water demand and need to be replenished by the upstream of the basin are referred to as the beneficiary areas, and those otherwise are called provision regions. With the combination of terrain gradients and human needs, water provision services always flow from provision areas to beneficiary areas. In 2015, the southern and eastern cities played the role of water service providers, especially Yongzhou and Chenzhou. Locations showing a high inflow of freshwater, such as Hengyang and Changsha, implied that they were part of the benefiting service area. The southern cities displayed the highest outflow among different regions, indicating that the high water-yield was a principal contributor to the high flow for these cities.

In general, water flow varies from -16.33 × 10^8 m^3 to 13.69 × 10^8 m^3 from upstream to downstream, which provides the possibility of reducing the spatial heterogeneity and promoting the equilibrium between water supply and demand. However, a water gap exists in cities after the natural confluence process, and artificial water intake or diversion is extremely necessary.

4 Discussion

4.1 Factors influencing the change in supply and demand of water provision services

In this study, we quantified the supply and demand of water provision services, and an obvious heterogeneity was observed. The results demonstrated that the average water production capacity and demand of northwest cities were generally lower than those of other cities, which are mainly affected by the topography of the basin, the level of urbanization, and grain for green plan (GFGP) (Deng et al. 2021a, Deng et al. 2021b). The construction of the Dongting Lake eco-economic circle and the integration of CZX, construction land,

and artificial landscape increased rapidly, resulting in a high average water yield capacity in the Yueyang and CZX urban agglomerations. Additionally, the hydrological characteristics of runoff changes are affected by changes in LUCC (Hurkmans et al. 2009; Maggi et al. 2010; Chen et al. 2020), which make natural landscapes such as woodlands and grasslands slow the formation of surface runoff by trapping precipitation and increasing infiltration. Many studies have shown that although the growth and development of a large area of artificial vegetation has controlled soil and water loss, it increases canopy interception and evapotranspiration, thus reducing surface water resources and water yield (Feng et al. 2016; Xu et al. 2018). However, the increase in surface runoff was closely linked to

the expansion of impermeable surfaces on urban construction sites, which resulted in faster hydrological responses (Song et al. 2015; Zhang et al. 2017). Although the total amount of water resources in the CZX urban agglomeration was relatively high, it should be pointed that the widespread impervious surface and drainage system in urban construction had caused the precipitation reaching the ground difficult to be directly used for production and living activities. Additionally, the expansion of urbanization has greatly increased the demand for urban residents and construction activities (Bryan et al. 2018; Wang et al. 2018). In 2015, the total amount of water consumption of the urban agglomeration reached 79.48×10^8 m³, which was close to the red line of water control. Among the
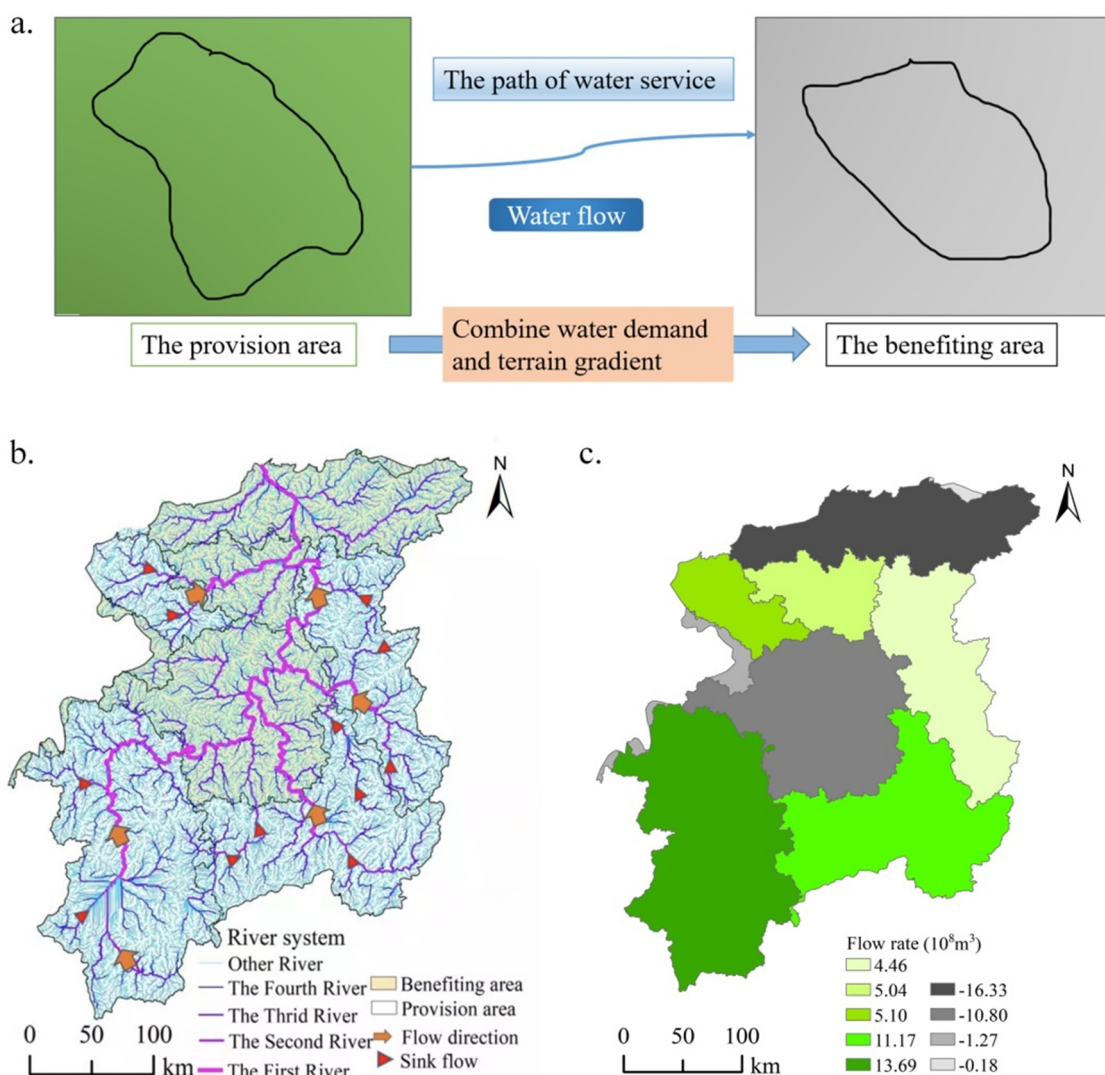

Fig. 5 The spatial flow of water provision services. (a) Schematic diagram of flow process; (b) Water provision services take the water system as a bridge and flows from the provision area to the benefiting area; (c) Flow rate of each administrative region. A positive water flow means that the water demand gap is satisfied after the natural confluence process, and there is no water demand gap. By contrast, a water gap exists in the cities.

cities, Changsha City (74.38%) had the highest level of urbanization (Appendix 1), but the per capita water resource consumption was only 1460 m^3. The utilization rate of water resources in Changsha and Xiangtan was only approximately 39% and 52%, respectively, and the pursuit of higher industrial added value (water consumption is 1.5 × the national average) has made the water quality standard rate of water function area in the CZX urban agglomeration less than 90%, which poses a threat to the water environment.

4.2 Changes of spatial matching in supply and demand of water provision services

It is gradually recognized that determining the spatial mismatch between supply and demand of ecosystem services is extremely important for decision-making management. In this study, the WSDR was used to analyze the spatial matching characteristics of the supply and demand of water provision services in the XRB. The results showed that in the downstream area mainly affected by rapid economic development, the supply–demand ratio of the CZX urban agglomeration was negative, indicating that the supply could not meet the demand to a certain extent. For example, the development and utilization rate of water resources (Appendix 2) in Xiangtan City was as high as 52.3%, and the IWC, UWC, and EWC were higher than their average levels. However, the lowest average annual precipitation cannot fully meet the needs of production and living, presenting a high risk of supply and demand. The WSDR was mainly affected by the GFGP in the upper reaches with abundant precipitation. For example, the storage capacities of large and medium-sized reservoirs (Appendix 3) in Chenzhou with a capacity of 70.89 × 10^8 m^3, 14.8% of the water resources development and utilization rate (Appendix 2), 50.34% of the urbanization level (Appendix 1), and a low population density of 1081 people/km^2 (Appendix 4) all contribute to a higher supply than demand. Therefore, it is necessary for water resources management to consider the spatial heterogeneity of supply and demand.

4.3 Influencing factors of spatial flow between water provision services supply and demand

Water resources have the characteristics of spatial flow. In this study, WSI and spatial mapping were used to determine the flow characteristics of water. Changsha, Shaoyang, Yueyang, and Hengyang were the main benefit areas (WSI < 0), which are closely related to the rapid development of the CZX urban agglomeration and the planning of the Dongting Lake Ecological Economic Zone. For example, Hengyang has developed industries, a water intake of 2.84 × 10^8 m^3 of industrial enterprises above the designated size, and a high population density (Appendix 4, Appendix 5) of 9,112 people/km^2, but the water production coefficient (Appendix 6), with a value of 0.53, was particularly low. Other regions were regarded as provisioning areas (WSI > 0), which were inseparable from the continuous implementation of the GFGP. At the same time, the area represented by the positive and negative WSI coincided with the WSDR, to a certain extent, which reflects the accuracy of the results. Changes in the form and magnitude of precipitation affected local water availability and supply (Daniel et al. 2016), aggravated the spatiotemporal distribution of water resources, brought about floods and drought (Piao et al. 2010, Uniyal et al. 2015, Shrestha et al. 2017), and seriously affected the sustainable development of the ecological economy. Therefore, it is important to optimize the allocation of water resources. Pinnate drainage patterns as scattered components of water conservancy projects, systems of canals, and groups of reservoirs in a basin can redistribute water resources in time and space to solve uneven problems (Peng et al. 2020), and water diversion projects are one of the important approaches to mitigate water shortages. Related research has shown that the combined action of the reservoir and canal systems reduces the balance gap between water supply and demand from 27.11% to 0.89%, and water supply capacity increased while water deficits decreased remarkably for diversion projects (Peng et al. 2020). For example, under the planning work situation of the eastern route of the South-to-North Water Diversion Project, the amount of water increased by 2,800 million m^3 even during the period of extreme drought (Zeng et al. 2020). Therefore, the construction of the Mangshan Reservoir could adjust the uneven spatial and temporal distribution through the flow of water resources, thus alleviating the contradiction between supply and demand of water resources in Hunan Province.

4.4 Limitations and suggestions

Although we have done our best to calculate the supply and demand of water provision services and simulate the water flow, this study also suffers from some limitations that should be addressed in future research. First, water service flow is influenced by various driving factors (Qin et al. 2019, Yang et al. 2019, Shi et al. 2020), and has complex and internal mechanisms. Owing to the limitations of data and methods, in service flow rendering, the natural confluence process flowing from upstream to downstream was considered. However, the influence of groundwater on water supply and the regulation function of human infrastructure such as dams, reservoirs, and water transfer projects on water resources have been ignored (Li et al. 2017, Xu et al. 2021). In the future, it will be necessary to strengthen the quantitative research of the effects of natural and human activities on the supply, demand, and flow of water provision services and clarify the driving mechanism of each factor. Meanwhile, under different and future scenarios, a new model considering more complex influence factors will be built to further simulate ecosystem service flows to reveal the comprehensive situations and strengthen water resource management. Second, this study only quantitatively estimated the supply and demand of water production services in the XRB in 2015. Because water provision services depend on natural ecology and human social processes at different time and space scales (Cui et al. 2019), the balance and spatial flow of water provision services are restricted and affected by temporal and spatial scales (Li et al. 2017, Li et al. 2021). In the future, it is necessary to study the water provision service on a variety of spatial and temporal scales, from the perspective of multiple interests, using multiple time dimensions and more refined spatial data to study the supply and demand changes and spatial flow patterns of water provision services.

5   Conclusion

To reduce water deficit and dislocation, our work used comprehensive methods to quantify the water supply and demand and their spatial flow. The spatial distribution trend of water supply and demand in the XRB was generally lower in the northwest than in other cities. With the advancement of urbanization and the implementation of GFGP, the contradiction between supply and demand of water resources of a typical urban agglomeration in the middle and lower reaches has become prominent, and there exists a mismatch between supply and demand in upstream cities. The results of mismatch between supply and demand and spatial flow of water provision services provide a basis for the rational allocation of regional resources and facilitate the construction of urban ecological compensation mechanisms. The management and control of water resource systems should be paid more attention, the construction of sponge cities increased, dynamic monitoring technologies strengthened, and a strategy of prioritizing the supply of water resources according to the degree of risk between supply and demand implemented in the future.

Electronic supplementary material: Supplementary material (Appendixes 1 to 6) is available in the online version of this article at https://doi.org/10.1007/s11629-021-6855-7

References

Allen R, Pereira L, Raes M, et al. (1998) Crop Evapotranspiration: Guidelines for Computing Crop Water Requirements, FAO Irrigation and Drainage Paper 56.

Bagstad KJ, Johnson GW, Voigt B, et al. (2013) Spatial dynamics of ecosystem service flows: a comprehensive approach to quantifying actual services. Ecosyst Serv 4: 117-125.
https://doi.org/10.1016/j.ecoser.2012.07.012

Bagstad KJ, Villa F, Batker D, et al. (2014) From theoretical to actual ecosystem services: mapping beneficiaries and spatial

flows in ecosystem service assessments. Ecol Soc 19(2): 64. https://doi.org/10.5751/ES-06523-190264

Baró F, Palomo I, Zulian G, et al. (2016) Mapping ecosystem service capacity, flow and demand for landscape and urban planning: a case study in the Barcelona metropolitan region. Land Use Pol 57: 405-417. https://doi.org/10.1016/j.landusepol.2016.06.006

Boithias L, Acuna V, Ziv G, et al. (2014) Assessment of the water supply: demand ratios in a Mediterranean basin under different global change scenarios and mitigation alternatives. Sci Total Environ 470-471(2): 567-577. https://doi.org/10.1016/j.scitotenv.2013.10.003

Brauman KA, Daily GC, Duarte TK, et al. (2007) The nature and value of ecosystem services: An overview highlighting hydrologic services. Annu Rev Env Resour 32: 67-98. https://doi.org/10.1146/annurev.energy.32.031306.102758

Bryan BA, Ye YQ, Zhang JE, et al. (2018) Land-use change impacts on ecosystem services value: Incorporating the scarcity effects of supply and demand dynamics. Ecosyst Serv 32: 144-157. https://doi.org/10.1016/j.ecoser.2018.07.002

Canadell J, Jackson RB, Ehleringer JB, et al. (1996) Maximum rooting depth of vegetation types at the global scale.

Chen DS, Li J, Yang XN, et al. (2020) Quantifying water provision service supply, demand and spatial flow for land use optimization: a case study in the YanHe watershed. Ecosyst Serv 43: 13. https://doi.org/10.1016/j.ecoser.2020.101117

Chen DS, Li J, Zhou ZX, et al. (2017) Simulating and mapping the spatial and seasonal effects of future climate and land-use changes on ecosystem services in the Yanhe watershed, China. Environ Sci Pollut Res 25: 1115-1131. https://doi.org/ 10.1007/s11356-017-0499-8

Cui FQ, Tang HP, Zhang Q, et al. (2019) Integrating ecosystem services supply and demand into optimized management at different scales: a case study in Hulunbuir, China. Ecosyst Serv 39: 17. https://doi.org/10.1016/j.ecoser.2019.100984

Daniel M, Lemonsu A, Viguié V. (2016) Role of watering practices in large-scale urban planning strategies to face the heat-wave risk in future climate. Urban Clim: S2212095516300505. https://doi.org/10.1016/j.uclim.2016.11.001

Deng CX, Zhu DM, Nie XD, et al. (2021a) Precipitation and urban expansion caused jointly the spatiotemporal dislocation between supply and demand of water provision service. J Environ Manage. 299: 113660. https://doi.org/10.1016/j.jenvman.2021.113660

Deng CX, Liu JY, Liu YJ, et al. (2021b). Spatiotemporal dislocation of urbanization and ecological construction increased the ecosystem service supply and demand imbalance. J Environ Manage 288: 112478. https://doi.org/10.1016/j. jenvman.2021.112478

Farley KA, Jobbágy EG, Jackson RB. (2005) Effects of afforestation on water yield: a global synthesis with implications for policy. Global Change Biol 11: 1565-1576. https://doi.org/10.1111/j.1365-2486.2005.01011.x

Feng XM, Fu BJ, Piao S, et al. (2016) Revegetation in China's Loess Plateau is approaching sustainable water resource limits. Nat Clim 11. https://doi.org/10.1038/NCLIMATE3092

Fischer G, Nachtergaele FO, Prieler S, et al. (2008) Global Agro-ecological Zones Assessment for Agriculture (GAEZ), IIASA.

Flach R, Ran Y, Godar J, et al. (2016) Towards more spatially explicit assessments of virtual water flows: linking local water use and scarcity to global demand of Brazilian farming commodities. Environ Res Lett 11(7). https://doi.org/10.1088/1748-9326/11/7/075003

FU BJ, Zhang LW, Xu ZH, et al. (2015) Ecosystem services in changing land use. J Soil Sediment 15: 833-843. https://doi.org/10.1007/s11368-015-1082-x

Hurkmans R, Terink W, Uijlenhoet R, et al. (2009) Effects of land use changes on streamflow generation in the Rhine basin. Water Resour Ees 45(6): 735-742. https://doi.org/10.1029/2008WR007574

Kenneth J, Bagstad KJ, Gary W, et al. (2013) Spatial dynamics of ecosystem service flows: A comprehensive approach to quantifying actual services. Ecosyst Serv 4: 117-125. https://doi.org/10.1016/j.ecoser.2012.07.012

Li DL, Wu SY, Liu LB, et al. (2017) Evaluating regional water security through a freshwater ecosystem service flow model: A case study in Beijing-Tianjian-Hebei region, China. Ecol Indic 81: 159-170. https://doi.org/10.1016/j.ecolind.2017.05.034

Li X, Sun W, Zhang D, et al. (2021) Evaluating water provision service at the sub-watershed scale by combining supply, demand, and spatial flow. Ecol Indic 127. https://doi.org/10.1016/j.ecolind.2021.107745

Liu JY, Liu ML, Tian HQ, et al. (2005) Spatial and temporal patterns of China's cropland during 1990-2000: An analysis based on Landsat TM data. Remote Sens Environ 98: 442-456.

Maggi Federico, Pallud Céline. (2010) Martian base agriculture: The effect of low gravity on water flow, nutrient cycles, and microbial biomass dynamics. Adv Space Res 46: 1257-1265. https://doi.org/10.1016/j.asr.2010.07.012

Nelson E, Mendoza G, Regetz J, et al. (2009) Modeling multiple ecosystem services, biodiversity conservation, commodity production, and tradeoffs at landscape scales. Front Ecol Environ 7: 4-11. https://doi.org/10.1890/ 080023

Palomo I, Martín-López R, Haines-Young R, et al. (2013) National Parks, buffer zones and surrounding lands: Mapping ecosystem service flows. Ecosyst Serv 4: 104-116. https://doi.org/10.1016/j.ecoser.2012.09.001

Peng F, Li K, Liang R, Yang S, et al. (2020) Positive effect of a canal system and reservoir group on the spatial-temporal redistribution of water resources in a pinnate drainage pattern. Sci Total Environ 744: 140855. https://doi.org/10.1016/j.scitotenv.2020.140855

Piao SL, Ciais P, Huang Y, et al. (2010) The impacts of climate change on water resources and agriculture in China. Nature 467: 43-51. https://doi.org/10.1038/nature09364

Qin KY, Liu JY, Yan LW, et al. (2019) Integrating ecosystem services flows into water security simulations in water scarce areas: Present and future. Sci Total Environ 670: 1037-1048. https://doi.org/10.1016/j.scitotenv.2019.03.263

Redhead JW, Stratford CK, Jones L, et al. (2016) Empirical validation of the InVEST water yield ecosystem service model at a national scale. Sci Total Environ 569-570: 1418-1426. https://doi.org/10.1016/j.scitotenv.2016.06.227

Schröter M, Barton DN, Remme RP, et al. (2014) Accounting for capacity and flow of ecosystem services: A conceptual model and a case study for Telemark, Norway. Ecol Indic 36: 539-551. https://doi.org/10.1016/j.ecolind.2013.09.018

Serna-Chavez HM, Schulp PM, Bodegom Van, et al. (2014) A quantitative framework for assessing spatial flows of ecosystem services. Ecol Indic 39: 24-33. https://doi.org/10.1016/j.ecolind.2013.11.024

Sharp R, Tallis HT, Ricketts T, et al. (2018) InVEST 3.6.0 User's Guide.

Shi Y, Shi D, Zhou L, et al. (2020) Identification of ecosystem services supply and demand areas and simulation of ecosystem service flows in Shanghai. Ecol Indic 115: 106418. https://doi.org/10.1016/j.ecolind.2020.106418

Song W, Deng XZ, Yuan Z, et al. (2015) Impacts of land-use change on valued ecosystem service in rapidly urbanized North China Plain. Ecol Model 318: 245-253. https://doi.org/10.1016/j.ecolmodel.2015.01.029

Shrestha NK, Du XZ, Wang JY, et al (2017) Assessing climate change impacts on fresh water resources of the Athabasca River Basin, Canada. Sci Total Environ 601: 425-440.

https://doi.org/10.1016/j.scitotenv.2017.05.013

Uniyal B, Jha M, Verma A. (2015) Assessing climate change impact on water balance components of a river basin using SWAT model. Water Resour Manag 29: 4767-4785. https://doi.org/10.1007/s11269-015-1089-5

Verhagen W, Kukkala AS, Moilanen A, et al. (2017) Use of demand for and spatial flow of ecosystem services to identify priority areas. Conserv Biol 31: 860-871. https://doi.org/10.1111/cobi.12872

Vigl LE, Depellegrin D, Paulo P, et al. (2017) Mapping the ecosystem service delivery chain: Capacity, flow, and demand pertaining to aesthetic experiences in mountain landscapes. Sci Total Environ 574: 422-436. https://doi.org/10.1016/jscitotenv.2016.08.209

Villamagna AM, Angermeier and Bennett EM. (2013) Capacity, pressure, demand, and flow: a conceptual framework for analyzing ecosystem service provision and delivery. Ecol Complex 15: 114-121. https://doi.org/10.1016/j.ecocom.2013.07.004

Wang Q, Xu YP, Wu L, et al. (2018) Spatial hydrological responses to land use and land cover changes in a typical catchment of the Yangtze River Delta region. Catena 170: 305-315. https://doi.org/10.1016/j.catena.2018.06.022

Xu J, Xiao Y, Xie GD, et al. (2021) How to coordinate cross-regional water resource relationship by integrating water supply services flow and interregional ecological compensation. Ecol Indic 126(15). https://doi.org/10.1016/j.ecolind.2021.107595

Xu XB, Yang GS, Tan Y, et al. (2018) Ecosystem services trade-offs and determinants in China's Yangtze River Economic Belt from 2000 to 2015. Sci Total Environ 634: 1601-1614. https://doi.org/10.1016/j.scitotenv.2018.04.046

Xu ZH, Wei HJ, Fan Weiguo, et al. (2018) Energy modeling simulation of changes in ecosystem services before and after the implementation of a Grain-for-Green program on the Loess Plateau-A case study of the Zhifanggou valley in Ansai County, Shaanxi Province, China. Ecosyst Serv 31: 32-43. https://doi.org/10.1016/j.ecoser.2018.03.013

Yang D, Liu W, Tang LY, et al. (2019) Estimation of water provision service for monsoon catchments of South China: applicability of the InVEST model. Landscape Urban Plan 182: 133-143. https://doi.org/10.1016/j.landurbplan.2018.10.011

Yan R, Zhang XP, Yan SJ, et al. (2018) Spatial patterns of hydrological responses to land use/cover change in a catchment on the Loess Plateau, China. Ecol Indic 92: 151-160. https://doi.org/10.1016/j.ecolind.2017.04.013

Zank B, Kenneth J, Bagstad KJ, et al. (2016) Modeling the effects of urban expansion on natural capital stocks and ecosystem service flows: a case study in the Puget Sound, Washington, USA. Landscape Urban Plan 149: 31-42. https://doi.org/10.1016/j.landurbplan.2016.01.004

Zhang L, Hickel K, Dawes W R, et al. (2004) A rational function approach for estimating mean annual evapotranspiration 40: 89-97. https://doi.org/10.1029/2003WR002710

Zhang LQ, Peng J, Liu YX, et al. (2017) Coupling ecosystem services supply and human ecological demand to identify landscape ecological security pattern: a case study in Beijing-Tianjin-Hebei region, China. Urban Ecosyst 20: 701-714. https://doi.org/10.1007/s11252-016-0629-y

Zeng C, Ma J, Cao M, et al. (2020) Modeling Water Allocation under Extreme Drought of South-to-North Water Diversion Project in Jiangsu Province, Eastern China. Front Earth Sci-Prc 8. https://doi.org/10.3389/feart.2020.541664

Zhou WZ, Liu GH, Pan JJ, et al. (2005) Distribution of available soil water capacity in China. J Geogr Sci 15: 3-12. (In Chinese) https://doi.org/10.1016/j.scitotenv.2019.03.263